Air velocity profiles and perceptive canopy interactions of airblast sprayers used in Pacific Northwest perennial specialty crop production

Anura P. Rathnayake[1,3], Abhilash K. Chandel[1,2], Mark J. Schrader[1,2], Gwen A. Hoheisel[1], Lav R. Khot[1,2]

(1. Center for Precision and Automated Agricultural Systems, Irrigated Agriculture Research and Extension Center, Washington State University, Prosser, WA, 99350, USA;

2. Department of Biological Systems Engineering, Washington State University, Pullman, WA, 99164, USA;

3. University of Arkansas at Pine Bluff, Pine Bluff, AR, 71601, USA)

Abstract: This study aim was to provide a data-driven understanding of air velocity profiles of four commercial airblast sprayers widely used in the Pacific Northwest (PNW) region of the United States. The Rear's Powerblast (S1) and Pakblast (S2), Turbomist 30P (S3), and Columbia Accutec (S4) were evaluated (without water) using the custom developed Smart Spray Analytical System (SSAS). Air velocity profiles and geometrical attributes (symmetry and uniformity) were characterized in two sides as well as at three horizontal distances from the air outlet (0.6, 1.5, and 2.1 m) of each sprayer. The air velocity profiles were analogized to vertical canopy zones of three typical perennial specialty crops (cherry, apple, and grapevine) to identify sprayer suitability. Air velocity differences between the two sides were majorly significant ($p < 0.05$) for selected sprayers with magnitudes higher on the right side for S1 and S4, and on the left side for S3, but insignificant ($p > 0.05$) for S2. Symmetry of air delivery pattern was very high for sprayers S1 (95% ± 3%, mean ± standard deviation), S2 (82% ± 6%), and S3 (83% ± 3%) compared to S4 (64% ± 14%), while uniformity was high for all sprayers (left: 51%–72%, right: 59%–73%). Overall, the current configuration of sprayer S2 would be suitable for spray applications in modified vertical shoot position grapevine or comparable short tree fruit canopies. Sprayers S1, S3, and S4 would be better suited for spray applications in fruiting zones of taller canopies such as central leader apple and steep leader trained cherry trees. The air delivery evaluations, as conducted in this study, would help in performing sprayer adjustments for efficient agrochemical applications on various perennial specialty crops and canopy architectures.

Keywords: perennial specialty crops; airblast sprayers; smart spray analytical system; air velocity patterns; symmetry; uniformity; sprayer adjustments

Citation: Rathnayake, A. P., A. K. Chandel, M. J. Schrader, G. A. Hoheisel, and L. R. Khot. 2022. Air velocity profiles and perceptive canopy interactions of commercial airblast sprayers used in Pacific Northwest perennial specialty crop production. Agricultural Engineering International: CIGR Journal, 24(1): 78-89.

1 Introduction

Airblast sprayers are widely used for agrochemical applications in perennial specialty crop production. Such sprayers typically rely on artificially generated air stream to carry spray droplets to the target canopy. Sprayer air velocities and their distribution patterns tend to impact spray deposition (Panneton and Piché, 2005), distribution (Matthews, 2000), off-target drift, and overall application

Received date: 2020-09-11 **Accepted date:** 2021-02-18

***Corresponding author: Lav R. Khot,** Associate Professor, Department of Biological Systems Engineering, Washington State University, Pullman, WA, USA. Tel: +1 509-335-5638. E-mail: lav.khot@wsu.edu.

efficiency (Pezzi and Rondelli, 2000; Dekeyser et al., 2013). Poorly directed airflow may increase operational costs and negative impacts on environment and human health (Khot et al., 2012; Kasner et al., 2018). Therefore, it is critical to understand sprayer air velocity to aid adjustments for optimized spray applications (Pai et al., 2009; Van de Zande et al., 2017; Kasner et al., 2018; Bahlol et al., 2020a).

Sprayer air velocity has been evaluated previously using 2D or 3D sonic anemometers. Delele et al. (2007) used air velocity measurements of a crossflow sprayer to develop a computational fluid dynamics model and to simulate airflow from sprayer operational settings. Importantly, this was an indirect method to understand sprayer air velocity and requires extensive field or outdoor evaluations. Khot et al. (2012) studied the variations of sprayer air velocities by adjusting air outlet area on a retrofit air-assisted precision sprayer. In a field study, García-Ramos et al. (2012) reported that the use of an additional axial fan forward of the spray tank on an airblast sprayer would increase the duration of on-canopy air presence. Recently, Gu et al. (2014) observed airflow variability caused by altering fan inlet diameter on a variable rate airblast sprayer. Above studies highlight the dependence of air velocities on sprayer designs, which subsequently influences the spray applications (Salcedo et al., 2015; Van de Zande et al., 2017) in pest management.

The majority of the studies above used fixed air velocity measurement units/sample locations, which may not allow derivation of complete air velocity profiles along the air outlet plane or associated crop heights due to low data resolutions. Such approaches may also restrict understanding crop or canopy-specific sprayer adjustments for real-time spray applications. Immobility of major laboratory or fixed air velocity measurement units may also lead to non-frequent, expensive and laborious evaluations (Stajnko et al., 2011). To alleviate such concerns, the Smart Spray Analytical System (SSAS) has been developed by Bahlol et al. (2020a, 2020b) for autonomous characterizations of air velocity profiles in air-assisted sprayers.

Although many of the above studies have been conducted at different sprayer settings, the range of studied sprayers was limited. In addition, crop-specific interpretations of the air velocity profiles were rarely available. Therefore, the aim of this study was to derive a data-driven understanding of air velocity patterns and adjustment potentials of widely used airblast sprayers in perennial specialty crop production management in the Pacific Northwest (PNW) region of the United States. Specific study objectives were to: (1) obtain air velocity profiles of four commercial orchard/vineyard sprayers at three distances along the outlet plane on either side of the sprayer using SSAS and (2) quantify air pattern symmetry, uniformity as well as velocity from selected sprayers on different vertical canopy zones of tree fruit and grapevine crops at modern orchard systems.

2 Materials and methods

2.1 Sprayers

Four commercial airblast sprayers (Figure 1 and Table 1), henceforth referred as S1 through S4, were selected for their high adaptation to tree fruit and berry crop production in the PNW region of the United States. These sprayers are unique in air delivery component designs but typically employ large fans or blowers to generate required airflow to propel liquid spray towards the crop canopy.

Sprayer S1 (Figure 1a) is equipped with a six-blade axial fan of diameter 0.84 m and uses an electronically activated clutch to engage with tractor power-take-off (PTO). The axial fan draws air through the rear of the sprayer and forces it out an inverted “U” shaped air outlet, concentric to the fan axis. Nozzle bodies are mounted about the air outlet on an inverted “U” shaped manifold such that exiting air can carry spray droplets along their original trajectory. This airflow arrangement is also present in Sprayer S2 (Figure 1b). Sprayer S2 also uses an electronically activated clutch for engaging with the tractor

PTO. The axial fan however, for S2, is a smaller eight-blade fan of diameter 0.71 m.

(a) (b) (c) (d)

Figure 1 Commercial airblast sprayers (a) S1, (b) S2, (c) S3, and (d) S4 evaluated in this study. Solid yellow outlines to the right of each sprayer show pertinent air outlets

Table 1 Specifications of airblast sprayers

Parameter	Sprayer			
	S1	S2	S3	S4
Model	Powerblast Pultank	Pakblast	Turbomist 30P	Columbia Accutec
Manufacturer	Rears Mfg.	Rears Mfg.	Slimline Mfg.	Blueline Mfg.
Fan type	axial	axial	turbine	centrifugal blower
Number of fan blades	6	8	10	-
Fan diameter (m)	0.84	0.71	0.76	0.41
Fan speed (rpm)	2074	2000	2200	2000
Fan rotation (from rear)	anticlockwise	anticlockwise	anticlockwise	anticlockwise
Air-outlet area (m^2)/ side	0.18	0.15	0.11	0.08
Tank capacity (L)	1514	378 (left+ right)	1514	757 (main) + 114 (mix)

Sprayer S3 (Figure 1c) has a ten-blade turbine fan of diameter 0.76 m and engages the tractor PTO using a slip clutch. Unlike S1 and S2, S3 has a front air inlet that draws air into the fan through perforations on top of the fan housing. S3 has separate air outlets for left and right sides with an eccentricity of 0.22 m, which can be partially rotated for air and spray delivery swath adjustments to accommodate a range of canopy heights. The air outlet on the right side is angled 20° towards the sprayer's rear while that on the left side is perpendicular to the sprayer axis. Spray nozzles are mounted along the leading edges of the air outlets.

Sprayer S4 (Figure 1d) is equipped with an interchangeable triangular-shaped head with a flattened peak resulting in three linear air outlets. It has a centrifugal blower fan of diameter 0.41 m driven indirectly by the tractor PTO through high-density shock absorbing belts. The blower, located at front, draws air from the left inlet through perforations in the fan housing and pushes air towards the outlets at rear. Similar to S1 and S2, the nozzle bodies are mounted directly in the midst of air exit.

2.2 Smart spray analytical system

The SSAS is a custom-developed vertical patternator (Figure 2) that autonomously measures both air velocity and spray volumes at numerous customizable heights ranging from 1.10–2.85 m above ground level (AGL). This customization allows for sprayer calibration across a variety of tree canopies and typical canopy zones. In this study, eight heights were set at 1.30, 1.52, 1.74, 1.96, 2.18, 2.40, 2.62, and 2.84 m AGL pertinent to typical specialty crop canopies in the PNW. The SSAS is instrumented with a single board computer (model: ATMEGA 2560, Sparkfun Electronics®, Boulder, CO, USA), a 2D sonic anemometer (model: DS2, Meter Group, Inc., Pullman, WA, USA) for measuring air velocity, and a spray droplet capturing unit connected to a reservoir enclosing a liquid

level sensor (model: eTape, Milone Technologies, Inc., Sewell, NJ, USA) to measure spray volume. Data is stored onboard the SSAS to a memory card as well as transmitted wirelessly to a remote computer for real time pattern visualizations.

Figure 2 Smart Spray Analytical System setup in a typical test configuration for autonomous sprayer air velocity evaluations (1: sonic anemometer, 2: system control and data logging unit)

2.3 Evaluation trials

The sprayer evaluations were conducted at the Washington State University, Center for Precision and Automated Agricultural Systems, Prosser, WA, in Fall 2019. The sprayers were operated without liquid spray in air-assist delivery mode for these trials. Experimental details are discussed in the following sections.

2.3.1 Weather

Outdoor weather was continuously monitored during sprayer evaluation trials (Table 2) using an all-in-one microclimate weather station (model: ATMOS 41, Meter Group, Pullman, WA). It was installed in an open area, 15 m away from the test location and 4 m AGL. The wind speed, wind direction, air temperature, and relative humidity parameters were logged onto a data logger (model: CR1000, Campbell Scientific, Inc., Logan, UT, USA) at 0.2 Hz. Wind speed varied within limits 0.04–5.23 m s^{-1} while wind direction, air temperature and relative humidity ranged 90–324°N, 14.3°C–28.7°C, and 31%–73%, respectively.

Table 2 Summary of weather parameters monitored during the sprayer evaluation trials

Sprayer and side		Distance from sprayer outlet (m)	Wind speed (m s^{-1})	Wind direction (mean ± SD, °N)	Air temperature (mean ± SD, °C)	Rel. humidity (mean ± SD, %)
S1	Left	0.6	1.56 – 3.50	215 ± 11	18.4 ± 0.3	43 ± 1
		1.5	0.93 – 3.86	196 ± 16	19.0 ± 0.4	42 ± 1
		2.1	0.83 – 4.35	187 ± 13	19.3 ± 0.5	41 ± 1
	Right	0.6	0.12 –3.33	164 ± 12	20.2 ± 0.6	38 ± 2
		1.5	0.22 – 3.25	207 ± 14	20.8 ± 0.7	36 ± 1
		2.1	0.49 – 3.16	110 ± 20	21.2 ± 0.5	35 ± 2
S2	Left	0.6	0.04 – 1.90	206 ± 19	19.0 ± 0.5	59 ± 2
		1.5	0.06 – 1.58	141±18	17.1 ± 0.4	69 ± 1
		2.1	0.64 – 2.49	306 ± 13	14.6 ± 0.3	72 ± 1
	Right	0.6	0.09 – 3.27	190 ± 24	25.1 ± 0.8	39 ±2
		1.5	0.15 – 2.24	248 ± 13	23.3 ± 0.5	46 ± 3
		2.1	0.21 – 2.15	212 ± 18	21.5 ± 0.6	51 ± 2
S3	Left	0.6	1.24 – 5.11	293 ± 18	17.7 ± 0.7	44 ± 4
		1.5	1.70 – 4.78	269 ± 21	16.8 ± 0.3	46 ± 3
		2.1	0.13 – 3.12	197 ± 22	15.4 ± 0.9	59 ± 6
	Right	0.6	0.42 – 3.44	306 ± 14	20.7 ± 0.9	46 ± 2
		1.5	1.15 – 4.58	290 ± 11	23.2 ± 0.4	42 ± 1
		2.1	1.06 – 5.23	283 ± 15	25.1 ± 0.4	39 ± 1
S4	Left	0.6	0.41 – 2.36	265 ± 19	22.1 ± 0.7	42 ± 2
		1.5	0.19 – 2.17	258 ± 18	24.6 ± 0.8	38 ± 1

	2.1	0.12 – 2.14	239 ± 21	28.0 ± 0.7	32 ± 1
	0.6	0.08 – 1.41	150 ± 16	21.0 ± 0.5	64 ± 3
Right	1.5	0.27 – 4.72	235 ± 15	25.3 ± 1.1	51 ± 3
	2.1	1.19 – 4.19	266 ± 20	26.1 ± 0.7	51 ± 2

2.3.2 Air velocity data acquisition

Each sprayer was parked on a flat concrete pad to ensure ground uniformity throughout the trials. The data collection protocol described by Bahlol et al. (2020a) was adapted. Since the aim of the study was to evaluate air velocity patterns along the outlet plane, the SSAS was positioned at three distances from the sprayer outlet (Figure 3), marked on both left and right sides (-2.1, -1.5, -0.6, 0.6, 1.5, and 2.1 m). Three replicative trials were conducted at each distance for all selected sprayers. The tractor PTO speed was maintained at 540 rpm. Air velocity measurements at each height were logged and visualized on a remote computer.

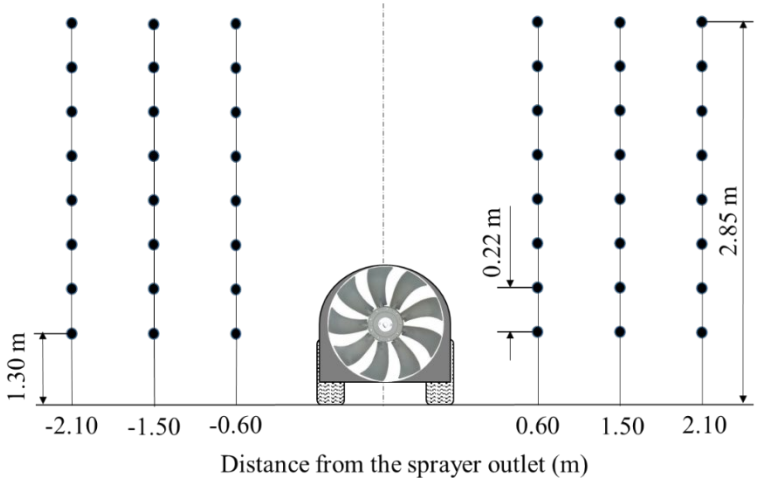

Figure 3 SSAS placement locations along sprayer outlet plane for air velocity pattern evaluations

2.4 Data analysis

Stored air velocity data in the memory card onboard-SSAS was transferred to a processing computer for further analysis. The velocity data did not follow a normal distribution (Shapiro-Wilk's test, $p > 0.05$) and showed skewness due to few outliers. A Wilcoxon's test was therefore conducted to assess the significance (5%) of differences in median air velocities between the left and right sides of the selected sprayers using RStudio software (Version 1.2.5, RStudio, Inc., Boston, MA, USA). A custom algorithm (MATLAB R2019a®, The Mathworks, Inc., Natick, MA, USA) was then used to generate interpolated air velocity contour profiles with respect to horizontal distance from sprayer air outlet and height AGL for both sides of the sprayers. Air velocity pattern geometry was interpreted using symmetry (*SYM*, %, Equation 1) and uniformity (*U*, %, Equations. 2 and 3) parameters. *SYM* defines air velocity similarity between two sprayer sides at same distance from outlet, while *U* is the air velocity similarity between heights at a given distance on a sprayer side (Farooq and Landers, 2004; Bahlol et al., 2020a).

$$SYM = 100 - \sum_{i=1}^{n} ABS\,(p_{il} - p_{ir}) \quad (1)$$

$$U(\%) = \frac{UI - \frac{1}{n}}{1 - \frac{1}{n}} \times 100 \quad (2)$$

$$UI = \frac{\sum_{i=1}^{n} \frac{q_i}{q_m}}{n} \quad (3)$$

Where, $ABS\ (p_{il} - p_{ir})$ is the absolute difference in the percent contribution of air velocities (p, %) at height i, for the total of measurements at all heights on the left (l) and right (r) sides. Parameter q_i is the air velocity (m s^{-1}) at height i, and q_m is the maximum air velocity (m s^{-1}) amongst all sampling heights (n) set to eight in this study.

Symmetry and uniformity have been categorized as low (0–25%), medium (25%–50%), high (50%–75%), and very high (75%–100%) (Farooq and Landers, 2004; Bahlol et al., 2020a). It must be noted that selected commercial sprayer units were not compared statistically for their air deliveries, as each has unique design features.

Mean air velocities in perspective of typical crops and architectures (Table 3, Figure 4) were also calculated. These include steep leader trained sweet cherry (*Prunus avium*), central leader trained apple (Gala, *Malus domestica*), and grapevine (Chardonnay, *Vitis vinifera*) with modified vertical shoot position (VSP) architecture. The cherry and apple canopies were divided into three zones and grapevine canopy was divided into two zones based on pertinent tree heights (Table 3). The means of air velocities measured in those zones were interpreted at 0.6 m distance from the outlet.

Table 3 Details of typical tree fruit canopies selected for sprayer air delivery interpretations

Parameter	Cherry	Apple	Grapevine
Architecture	Steep leader	Central leader	Modified VSP
Growth stage (BBCH scale)	91	71	81
Average height (m)	4.4	3.6	2
Average canopy width (m)	3	1.2	1.1
Row spacing (m)	5.5	3.0	2.4
Bottom zone (m AGL)	1.1–2.2	0.6–1.6	1–1.5
Middle zone (m AGL)	2.2–3.3	1.6–2.6	-
Top zone (m AGL)	3.3–4.4	2.6–3.6	1.5–2.0

Note: BBCH: Biologische Bundesanstalt, Bundessortenamt and Chemical industry.

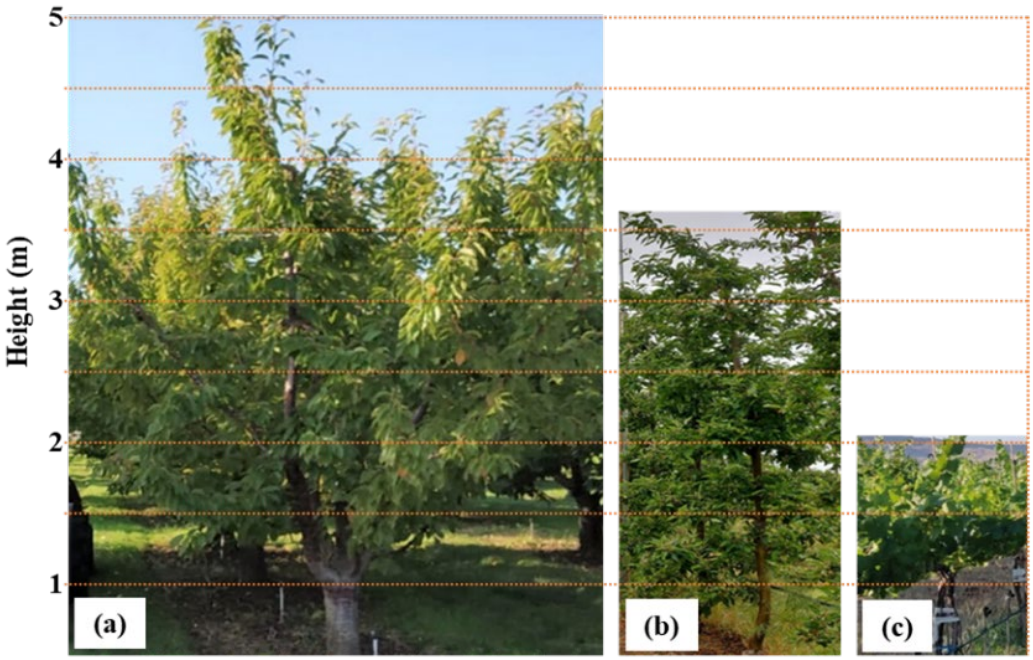

Figure 4 Canopy architectures typical to (a) sweet cherry, (b) apple, and (c) grapevine

3 Results and discussion

3.1 Air velocity profiles

The SSAS-assessed air velocity profile for sprayer S1 (Figure 5a) showed that velocities on the right side (range: 4.85–20.67 m s^{-1}, median: 8.64 m s^{-1}, mean: 9.68 m s^{-1}, standard deviation (SD): 3.63 m s^{-1}) were significantly higher (W-stat = 1242.5, $p < 0.01$) than those on the left side (range: 3.76–19.80 m s^{-1}, median: 5.67 m s^{-1}, mean: 7.42 m s^{-1}, SD: 4.30 m s^{-1}). This difference can be attributed to the anticlockwise rotation of the axial fan. As the fan blades rotate from left to right, there is a brief interruption in air outlet, causing high air forced out on the

right side. The relatively high contour density observed near the outlets indicates higher velocity change rates. The upward persistence of delivered air observed beyond 1.5 m on the right side, may contribute to off-target drift. Conversely, the horizontal persistence of delivered air observed on the left side (~20 m s^{-1} at 1.30–1.75 m AGL) may contribute to enhanced canopy penetration of spray delivered to the canopy zones of various crops and architectures (Panneton et al., 2005; Khot et al., 2012). Air velocity magnitudes for S1 were marginally different from those reported by Bahlol et al. (2020a) as the current evaluation was conducted in outdoor conditions, such that prevailing weather condition may influence sprayer air delivery.

Air velocities from sprayer S2 (Figure 5b) on the left side (range: 2.66–14.26 m s^{-1}, median: 4.54 m s^{-1}, mean: 5.91 m s^{-1}, SD: 2.92 m s^{-1}) differed insignificantly (W-stat = 2053.5, $p > 0.05$) from those on the right side (range: 1.01–14.95 m s^{-1}, median: 4.06 m s^{-1}, mean: 5.18 m s^{-1}, SD: 3.36 m s^{-1}). The contour profiles for S2 show a horizontal persistence of air on the right side while there is a slight downward persistence on the left. The downward persistence observed on the left side is unique to S2, likely because of the small fan size and low air intake capacity. These attributes also caused the air velocities pertinent to S2 to be relatively lower than that of S1. Intense velocities up to 1.5 m AGL which decrease with increasing height and distance from air outlet suggests efficient spray applications for shorter canopies (height < 2 m) and the need for potential adjustments for taller tree canopies.

Air velocities for sprayer S3 (Figure 5c) showed a significant difference (W-stat = 1401, $p < 0.05$) between the left (range: 4.16–17.41 m s^{-1}, median: 7.43 m s^{-1}, mean: 7.67 m s^{-1}, SD: 3.84 m s^{-1}) and the right side (range: 2.79–15.64 m s^{-1}, median: 5.20 m s^{-1}, mean: 5.31 m s^{-1}, SD: 2.82 m s^{-1}). Unlike S1 and S2, which had axial fans, sprayer S3 uses a turbine fan. The unique offset outlet design, which places the left outlet closer to the fan and in natural path of anticlockwise rotation could have caused more air to escape on the left side. Meanwhile, before exiting the right side, the air passes through an extra bend causing extra turbulence. This unique offset could be the cause for the observed delivery of significantly ($p < 0.05$) higher velocities to the left side compared to the right side of S3. The air velocity profiles for S3 on both sides were observed to first propagate horizontally and then vertically. While the velocity magnitudes were higher on the left side, contours show more uniform profiles on the right side with increasing distance. Another unit with the same make and model as S3 was also evaluated by Bahlol et al. (2020a) who reported comparatively different profiles as well as lower air velocities in controlled environmental conditions.

In the case of S4 (Figure 5d), air velocities on the left side (range: 0.84–16.41 m s^{-1}, median: 4.44 m s^{-1}, mean: 6.13 m s^{-1}, SD: 5.01 m s^{-1}) were significantly lower (W-stat = 1651, $p < 0.05$) than those on the right side (range: 1.31–16.14 m s^{-1}, median: 8.50 m s^{-1}, mean: 8.61 m s^{-1}, SD: 4.07 m s^{-1}). The contour profiles show potentially higher spray penetration on right side compared to the left side. The upward propagation of air delivery at 1.5 m distance from the sprayer outlet and beyond 2.5 m AGL is likely due to air exiting the top outlet. Such profiles may be caused by a centrifugal vacuum created on the left side causing higher air exit to the right. Moreover, the air outlet area of S4 is the smallest of all four sprayers, which could have contributed to higher exit velocities and turbulent profiles. This turbulence results in pockets of increased air velocity as observed at 2.50–2.75 m AGL.

Overall, the spray (plant protection products) deposition is affected by three major factors; prevailing weather, canopy physiology, and spray application equipment. Under recommended limits of weather parameters and in managed orchard systems, the air velocity profiles (Figure 5) potentially depict the trajectories of spray droplet penetration and deposition (Panneton and Piché, 2005; Endalew et al., 2010). Nonetheless, these deposition and penetration characteristics may vary subject to liquid spray and nozzle configurations of the sprayer.

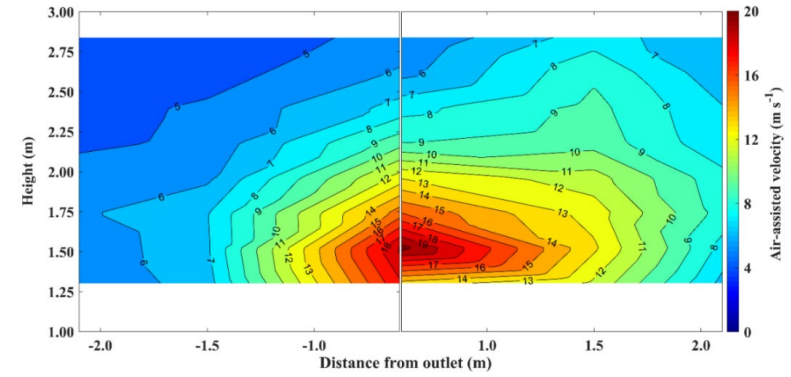
Height (m)
Distance from outlet (m)
Air-assisted velocity (m s-1)

(a)

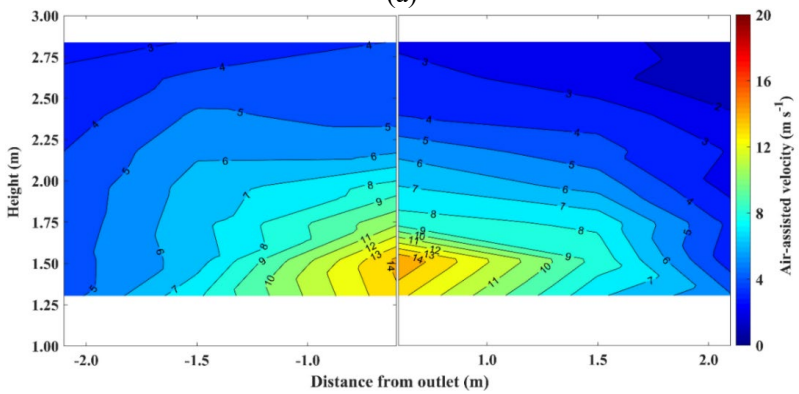
Height (m)
Distance from outlet (m)
Air-assisted velocity (m s-1)

(b)

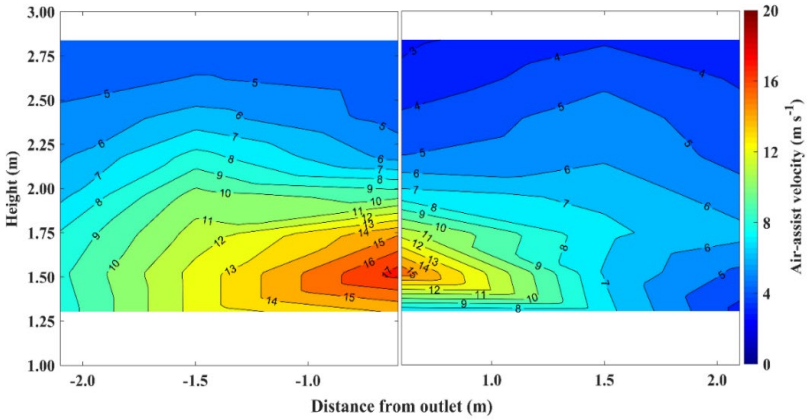
Height (m)
Distance from outlet (m)
Air-assist velocity (m s-1)

(c)

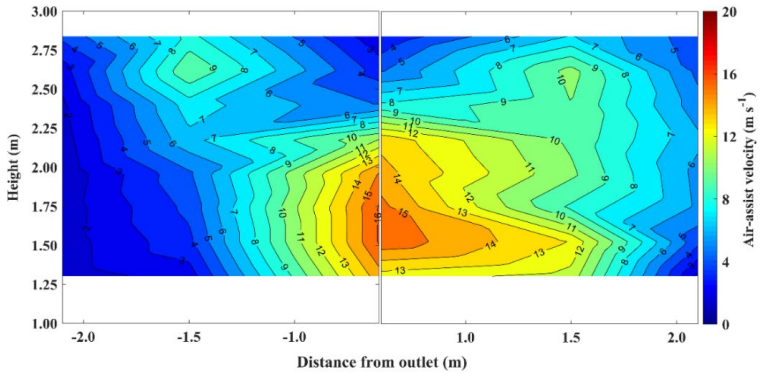
Height (m)
Distance from outlet (m)
Air-assist velocity (m s-1)

(d)

Figure 5. Air velocity patterns along the outlet plane with respect to height and distance from outlet of sprayers (a) S1, (b) S2, (c) S3, and (d) S4. Negative and positive distances indicate left and right sides, respectively.

3.2 Pattern symmetry and uniformity

All sprayers had a very high symmetry (Figure 6a) at 0.6 m, i.e. 90%, 89%, 85%, and 84% for S1, S2, S3, and S4, respectively. At 1.5 and 2.0 m from the outlet, symmetry for S1 (97% and 97%), S2 (79% and 76%), and S3 (86% and 80%), remained very high, while that for S4 reduced to high (56% and 52%). Observations showed no symmetry variation (very high) with distance for sprayers S1, S2, and S3 while showing a slight variation for S4 (very high to high). Symmetric air patterns suggest potentially consistent spray applications by both sides of evaluated sprayers.

Uniformity of air velocities of selected sprayers are shown in figure 6b. For S1, uniformity on the left side increased from high to very high with distances of 0.6 (55%), 1.5 (79%), and 2.1 m (82%) from the outlet. Similarly, uniformities on the right side increased from medium to very high with distance of 0.6 (49%), 1.5 (77%), and 2.1 m (82%). Uniformity differences between the two sides at 0.6 m could be attributed to previously discussed air velocity magnitude differences. For S2, uniformity on the left side increased from high at 0.6 (52%) and 1.5 m (69%) to very high at 2.1 m (83%) from the air outlet. Meanwhile, the uniformity on the right side of S2 increased from medium at 0.6 m (43%) to high at 1.5 m (55%) and very high at 2.1 m (80%). These differences may result in inhomogeneous spray coverage and depositions.

Air pattern uniformity for S3 increased from medium at 0.6 m (47%) to high at 1.5 m (67%) and 2.1 m (70%) from air outlet on the left side. On the right side, uniformity increased from high at 0.6 m (56%) to very high at 1.5 m (80%) and 2.1 m (83%), which also was reflected by wide contour profiles (Figure 5b). Similar to S1 and S2, uniformity differences between the two sides could be due to the observed differences in air velocities. Additionally, air pattern symmetry and uniformity for S1 and S3 showed different trends compared to those in controlled conditions (Bahlol et al., 2020a). This may be because in a controlled environment, there could be a significant interference between the suction and delivery air for same source and sink elements in absence of external wind. Whereas, when operating in outdoor conditions, there exists minimum dependency between source and sink amounting to a minimal interference between the suction and delivered air. Presence of external wind may also affect the dynamics of sprayer's air delivery. Furthermore, sprayer S3 in this study was a different unit than that evaluated by Bahlol et al. (2020a) and pertinent observations suggest that every individual unit may perform differently irrespective of the same make and model even with insignificant differences in design parameters (Czaczyk et al., 2015).

For sprayer S4, neither side had very high air pattern uniformity. A peculiar uniformity reduction from high at 0.6 m (60%) and 1.5 m (54%) to medium at 2.1 m (38%) was observed with increasing distance from outlet. This uniformity reduction might have been caused by the air turbulence observed uniquely in S4 (Figure 5d). On the right side, uniformity category remained unchanged from high at 0.6 (66%), 1.5 (74%) and 2.1 m (73%) distance from outlet. Such inconsistencies between sprayer sides were also reflected in the velocity contour profiles and pattern symmetry suggesting configuration adjustment needs for effective spraying.

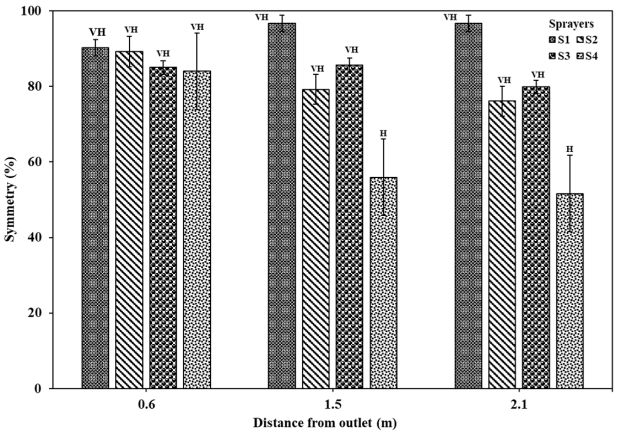

(a)

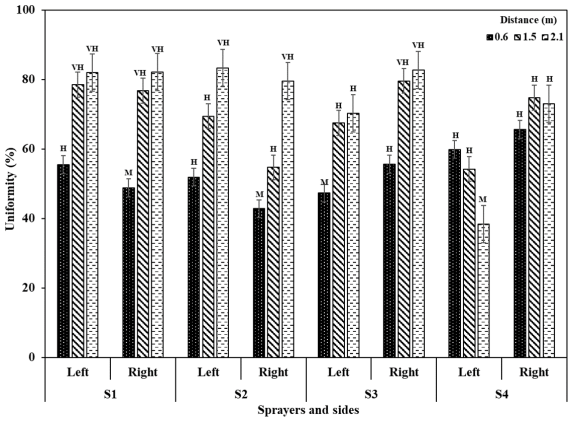

(b)

Figure 6 Air velocity (a) symmetry, and (b) uniformity on two sides for selected sprayers (mean ± standard error) at different distances from outlet

3.3 Sprayer suitability to typical crop canopies

As per selected crop canopies, air velocities of evaluated sprayers showed decreasing trends from bottom to top zones (Figures 5 and 7) indicating sufficient spray delivery potentials at bottom–middle fruiting zones (Bayat et al., 1994; Wenneker et al., 2009; Duga et al., 2015). As per cherry canopy (Figure 4a), delivered mean air velocities (Figure 7a) to the bottom–middle zones were highest for sprayer S1, followed by S4, S3, and S2. As per apple canopy zones (Figures 4b and 7b), highest mean air velocities were recorded for sprayer S1, followed by S4, S3, and S2. With respect to selected grapevine canopies (Figures 4c and 7c), sprayer S1 delivered air at the highest mean velocity followed by S4, S3, and S2. The differences in air velocities pertinent to canopy zones can be visualized on the contour plots as velocity distribution along the height AGL (Figure 5).

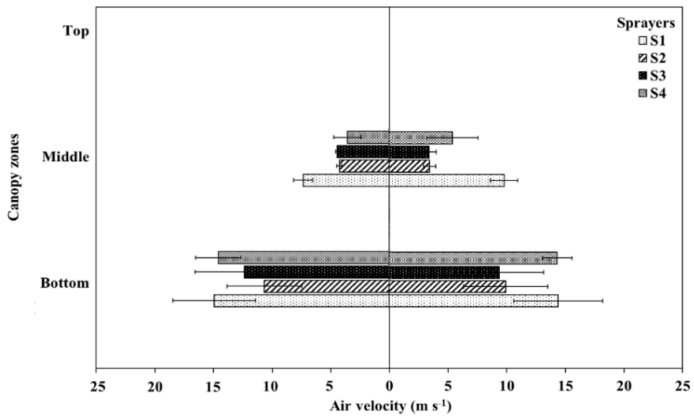

(a)

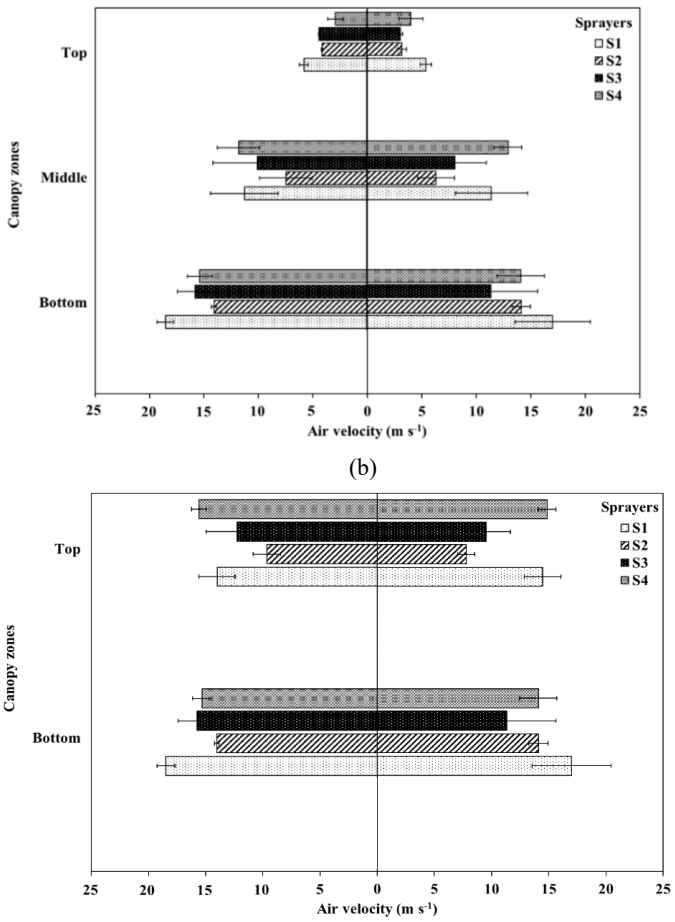

(b)

(c)

Figure 7 Mean delivered air velocities (with standard deviation as error bars) from selected sprayers pertinent to canopy zones of typical (a) cherry, (b) apple, and (c) grapevine crops

As per observed air patterns and profiles, sprayers S1, S3, and S4 would suit for spray applications in apple canopies and potentially in cherry canopies with slight sprayer adjustments. The current configuration of sprayer S2 may be well suited for spray applications on grapevines but might not generate enough air to supply sufficient spray to high-density cherry canopies and some top–middle zone sections of apple canopies. Higher velocity magnitudes from S1, S3, and S4 may ensure high spray penetration into grapevine canopies but may also contribute to potentially high drift (Grella et al., 2017; Kasner et al., 2018; Sinha et al., 2019). Switching off the top nozzles and adjustment of air delivery outlets (i.e. deflector plates) or the fan speed may minimize such spray drift potentials.

4 Conclusions

The data-driven approach provided insights on discrete air velocity profiles for selected airblast sprayers at default settings, which could be attributed to uniqueness of their air delivery component designs. Significant differences were observed between the delivered air velocities on the left and right sides for majority of selected sprayers ($p < 0.05$). Sprayer S1 had a very high symmetry in air velocity patterns on the left and right sides with medium to high range of uniformity. Sprayer S2 had comparatively lower velocity magnitudes but very high symmetry and increased uniformity with distance from air outlet. Rapid and turbulent air velocity patterns of S3 resulted in medium to high range of uniformity near the sprayer outlet but consistently very high symmetry along the sprayer air outlet. Turbulence from the centrifugal fan of S4 could have reduced symmetry from very high to high and uniformity from high to medium levels along the outlet.

Since the fruiting and foliar zones majorly range from upper-bottom to lower-top canopy zones, current operational settings of sprayers S1, S3, and S4 make them suitable for spray applications in taller to shorter canopy heights such as apple, cherry, grapevines and blueberry crops. However, additional adjustments would be needed for reducing off-target drift losses. The air delivery profiles of sprayer S2 would exclusively fit spray applications in shorter canopies, i.e., grapevines and blueberry. Customizable height ranges on the SSAS could also provide enhanced air-assist behavior understanding for the test sprayers. Additionally, possible air delivery adjustment solutions could be explored for selected sprayer types for efficient canopy and growth stage specific spray applications. This data-driven study will help develop databases to identify the best sprayer operational configurations for growers. Researchers, manufacturers and spray-related industries may also use such data for design optimizations and efficient spraying.

Acknowledgements

This study was funded in part by the Washington State Tree Fruit Research Commission (WTFRC), the USDA Forest Services and WMPN0745 projects. Authors thank Dr. Haitham Bahlol and Mr. Patrick Scharf for their technical support and Mr. Tory Schmidt and Mr. Gerardo Garcia from WSTFRC for providing Rears Pakblast and Columbia Accutec sprayers. Authors also thank Slimline Mfg. for providing the Turbomist 30P sprayer for the study.

Conflict of interest

The authors declare no conflict of interest.

References

Bahlol, H. Y., A. K. Chandel, G. A. Hoheisel, and L. R. Khot. 2020a. The smart spray analytical system: Developing understanding of output air-assist and spray patterns from orchard sprayers. *Crop Protection*, 127: 104977.

Bahlol, H. Y., A. K. Chandel, G. A. Hoheisel, and L. R. Khot. 2020b. Smart spray analytical system for orchard sprayer calibration: a proof of concept and preliminary results. *Transactions of the ASABE*. 63(1): 29-35.

Bayat, A., Y. Zeren, and M. R. Ulusoy. 1994. Spray deposition with conventional and electrostatically-charged spraying in citrus trees. *Agricultural Mechanization in Asia Africa and Latin America*, 25(4): 35-39.

Czaczyk, Z., G. Bäcker, R. Kelcher, and R. Müller. 2015. Air flow characteristics-proposed as mandatory requirement for airblast sprayers. *Julius-Kühn-Archiv*, 449: 168.

Dekeyser, D., A. T. Duga, P. Verboven, A. M. Endalew, N. Hendrickx, and D. Nuyttens. 2013. Assessment of orchard sprayers using laboratory experiments and computational fluid dynamics modelling. *Biosystems Engineering*, 114(2): 157-169.

Delele, M.A., Jaeken, P., Debaer, C., Baetens, K., Endalew, A.M., Ramon, H., Nicolaï, B.M. and Verboven, P. 2007. CFD prototyping of an air-assisted orchard sprayer aimed at drift reduction. Computers and Electronics in Agriculture, 55(1): 16-27.

Duga, A. T., K. Ruysen, D. Dekeyser, D. Nuyttens, D. Bylemans, B. M. Nicolai, and P. Verboven. 2015. Spray deposition profiles

in pome fruit trees: Effects of sprayer design, training system and tree canopy characteristics. *Crop Protection*, 67: 200-213.

Endalew, A. M., C. Debaer, N. Rutten, J. Vercammen, M. A. Delele, H. Ramon, B. M. Nicolaï, and P. Verboven. 2010. Modelling pesticide flow and deposition from air-assisted orchard spraying in orchards: a new integrated CFD approach. *Agricultural and Forest Meteorology*, 150(10):1383-1392.

Farooq, M. and Landers, A.J. 2004. Interactive effects of air, liquid and canopies on spray patterns of axial-flow sprayers. In 2004 ASAE Annual Meeting (p. 1). American Society of Agricultural and Biological Engineers.

García-Ramos, F. J., M. Vidal, A. Boné, H. Malón, and J. Aguirre. 2012. Analysis of the air flow generated by an air-assisted sprayer equipped with two axial fans using a 3D sonic anemometer. *Sensors*, 12(6): 7598-7613.

Grella, M., M. Gallart, P. Marucco, P. Balsari, and E. Gil. 2017. Ground deposition and airborne spray drift assessment in vineyard and orchard: The influence of environmental variables and sprayer settings. *Sustainability*, 9(5):728.

Gu, J., H. Zhu, W. Ding, and X. Wang. 2014. Characterization of air profiles impeded by plant canopies for a variable-rate air-assisted sprayer. *Transactions of the ASABE*, 57(5): 1307-1315.

Kasner, E. J., R. A. Fenske, G. A. Hoheisel, K. Galvin, M. N. Blanco, E. Y. Seto, and M. G. Yost. 2018. Spray drift from a conventional axial fan airblast sprayer in a modern orchard work environment. *Annals of Work Exposures and Health*, 62(9): 1134-1146.

Khot, L. R., R. Ehsani, G. Albrigo, P. A. Larbi, A. Landers, J. Campoy, and C. Wellington. 2012. Air-assisted sprayer adapted for precision horticulture: spray patterns and deposition assessments in small-sized citrus canopies. *Biosystems Engineering*, 113(1): 76-85.

Matthews, G. A. 2000. A review of the use of air in atomisation of sprays, dispersion of droplets down wind and collection on crop foliage. *Aspects of Applied Biology*, 57: 21-27.

Pai, N., M. Salyani, and R. D. Sweeb. 2009. Regulating airflow of orchard airblast sprayer based on tree foliage density. *Transactions of the ASABE*, 52(5): 1423-1428.

Panneton, B., and M. Piché. 2005. Interaction between application volume, airflow, and spray quality in air-assisted spraying. *Transactions of the ASAE*, 48(1): 37-44.

Panneton, B., B. Lacasse, and M. Piché. 2005. Effect of air-jet configuration on spray coverage in vineyards. *Biosystems Engineering*, 90(2): 173-184.

Pezzi, F., and V. Rondelli. 2000. The performance of an air-assisted sprayer operating in vines. *Journal of Agricultural Engineering Research*, 76(4): 331-340.

Salcedo, R., R. Granell, G. Palau, A. Vallet, C. Garcerá, P. Chueca, and E. Moltó. 2015. Design and validation of a 2D CFD model of the airflow produced by an airblast sprayer during pesticide treatments of citrus. *Computers and Electronics in Agriculture*, 116: 150-161.

Sinha, R., R. Ranjan, L. R. Khot, G. A. Hoheisel, and M. J. Grieshop. 2019. Drift potential from a solid set canopy delivery system and an axial–fan air–assisted sprayer during applications in grapevines. *Biosystems Engineering*, 188: 207-216.

Stajnko, D., P. Vindis, and B. Mursec. 2011. Automated system for targeted spraying in orchards by using RGB imaging. In *DAAAM International Scientific Book 2011*, Vol. 10, ch. 23, 283-301. January, 2011.

Van de Zande, J. C., M. Schlepers, J. W. Hofstee, J. G. P. Michielsen, and M. Wenneker. 2017. Characterization of the air flow and the liquid distribution of orchard sprayers. In *14th Workshop on Spray Application in Fruit Growing*, 41-42. Hasselt, Belgium, 9-13 May.

Wenneker, M., J. C. Van de Zande, and M. Poulsen. 2009. Effect of nozzle type on pesticide residues on fruits. In *SuproFruit 2009 10th Workshop on Spray Application Techniques in Fruit Growing*, 30-31. Wageningen, the Netherlands, 30 September-2 October.